Braz J Phys (2015) 45:234–237
DOI 10.1007/s13538-015-0307-1

CONDENSED MATTER

Electrical Resistivity in Non-stoichiometric MoO_2

L. M. S. Alves · S. S. Benaion · C. M. Romanelli · C. A. M. dos Santos · M. S. da Luz · B. S. de Lima · F. S. Oliveira · A. J. S. Machado · E. B. Guedes · M. Abbate · R. J. O. Mossanek

Received: 30 October 2014 / Published online: 24 February 2015

Abstract MoO_y with $1.85 \leq y \leq 2.20$ has been studied by X-ray diffractometry and photoemission spectroscopy at room temperature and by electrical resistance as a function of temperature from 2 to 300 K. Although X-ray diffractograms are very similar to the stoichiometric MoO_2 with monoclinic structure of the space group $P2_1/c$ (14), the electrical properties are strongly dependent on the oxygen composition. Samples with $y=1.85$ and 1.90 show anomalous behavior in electrical conductivity. Photoemission and X-ray absorption spectroscopy measurements suggest that this anomalous behavior is related to the presence of Mo^{3+} ions such as in K_xMoO_2 compound.

Keywords Oxides · Photoelectron spectroscopy · Electrical properties

1 Introduction

Molybdenum oxides are well known due to the great stoichiometric and physical properties variety [1–3]. The ideal molybdenum dioxide bulk is monoclinic, weakly paramagnetic, and display a conventional metal-like behavior [4]. Theoretical studies have shown that ultrathin films [5] and bulk with some molybdenum or oxygen vacancies can form magnetic moment with ferromagnetic couple. The origin of magnetism is still under investigation, but some authors believe that the reason may be due to defects such as vacancies or interstitial doping [6, 7]. These results indicate that small fluctuations of the Mo valences can cause considerable changes in the physical properties of the MoO_y samples.

Considering y between 2 and 3, it is possible to find phases with very different physical properties. MoO_2 has asymmetric crystalline structure with Mo-Mo channels along the c-axis, which results in anisotropic conductivity [8, 9]. Molybdenum trioxide in its more stable phase is orthorhombic and insulator [10, 11]. Furthermore, other binary molybdenum oxides are reported with different chemical composition and Mo valences, such as the Magnéli phases Mo_4O_{11}, Mo_8O_{23}, and Mo_9O_{26}. All phases are very interesting due to their physical properties such as quasi-low-dimensional electrical conductivity and formation of charge density wave (CDW) instabilities [8, 9, 12–14].

Many other molybdenum oxides have metal-metal bonds in the structure forming easy conduction along one direction. $Li_{0.9}Mo_6O_{17}$ [15] and $K_{0.3}MoO_3$ [16, 17] are some good examples. These compounds form monoclinic structures and are reported to be highly anisotropic with quasi-one- or quasi-two-dimensional electrical behavior [3]. The electrical resistance of $Li_{0.9}Mo_6O_{17}$ has been well described by two-band Luttinger liquid (LL) with two power-law T terms [18]. K_xMoO_2 has an anomalous metallic behavior below 70 K which can be described by one LL power-law temperature term [19, 20]. Besides the high anisotropic behavior of these compounds, they show other interesting physical properties. For instance, $Li_{0.9}Mo_6O_{17}$ undergoes a metallic-to-semiconducting transition at 28 K and surprisingly changes from semiconducting-like behavior to superconducting below 1.9 K [21]. K_xMoO_2 superconducts with critical temperature

L. M. S. Alves (✉) · S. S. Benaion · C. M. Romanelli · C. A. M. dos Santos · M. S. da Luz · B. S. de Lima · F. S. Oliveira · A. J. S. Machado
Escola de Engenharia de Lorena, Universidade de São Paulo, Lorena, SP 12600-970, Brazil
e-mail: leandro_fisico@hotmail.com

M. S. da Luz
Instituto de Ciências Tecnológicas e Exatas, Universidade Federal do Triângulo Mineiro, Uberaba, MG 38064-200, Brazil

E. B. Guedes · M. Abbate · R. J. O. Mossanek
Departamento de Física, Universidade Federal do Paraná, Curitiba, PR 81531-990, Brazil

(T_C) ranging from 4 to 10 K depending on the sample composition [19, 20]. In a recent paper, superconductivity was found at 12 K in oxygen-deficient MoO_2 [22].

In this work, the influence of the oxygen contents on the electrical behavior of the MoO_y samples with y near 2 is reported. The results show that the presence of the Mo^{3+} ions in the MoO_y samples is responsible for a variety of electrical behavior. An anomalous electrical behavior similar to the power-law temperature dependence of K_xMoO_2 compound has been observed in the $MoO_{1.85}$ and $MoO_{1.90}$ samples. These results suggest that K-doping is not necessary for inducing the anomalous electrical behavior observed in K_xMoO_2 [19, 20].

2 Experimental

Polycrystalline samples of MoO_y with $1.85 \leq y \leq 2.20$ were prepared by solid state diffusion method. Samples containing appropriate amounts of oxygen (y) were prepared by mixing MoO_3 and Mo metallic. The mixtures were compacted into pellets, placed in quartz tubes under vacuum, and heat treated at 400 °C for 1 day followed by 700 °C for 3 days. X-ray powder diffraction patterns were performed at room temperature using a Shimadzu diffractometer (XRD 6000) with 40 kV–30 mA, Cu-Kα radiation, and Ni filter. The 2θ data were collected from 10 to 90° using a step of 0.05°. X-ray photoemission (XPS) and absorption (XAS) spectroscopies were performed in the soft X-ray (SXS) and spherical grating monochromator (SGM) beamlines, respectively, at Laboratório Nacional de Luz Síncroton (LNLS, Campinas, SP, Brazil). Both measurements were performed at UHV, with a base pressure of around 10^{-9} mbar, and at room temperature. The overall energy resolution was about 0.4 eV ($h\upsilon$ = 1840 eV) for XPS and 0.5 eV for XAS spectra. Electrical resistance as a function of temperature was measured using standard four-probe method in a 9T Physical Properties Measurement System (PPMS) from 2 to 300 K.

3 Results

Figure 1 displays X-ray diffraction (XRD) patterns for samples in the composition range of $1.85 \leq y \leq 2.20$.

Samples with y ranging from 1.85 to 2.05 are single phase within the resolution of the XRD technique. On the other hand, samples with higher oxygen contents ($y \geq 2.05$) clearly show impurity phases (indicated by arrows). Based upon these results, we can study the physical properties of the single-phase samples in the MoO_y system within the solubility limit. Due to several oxygen compositions of the samples, different physical properties are expected. This has attracted great attention nowadays to the MoO_2 film or bulk samples as reported by some authors [5, 6].

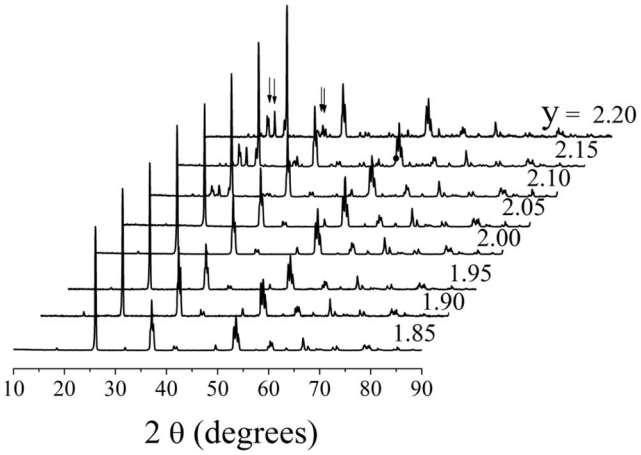

Fig. 1 X-ray diffraction patterns for the MoO_y samples ($1.85 \leq y \leq 2.20$). For $y \geq 2.10$, additional peaks, which can be related to orthorhombic Mo_4O_{11} structure, are observed [23] (see, for instance, peaks indicated by *arrows* for y=2.20)

XRD has also been studied by Rietveld refinement. Experimental X-ray diffractometry data for the $MoO_{2.05}$, the final Rietveld refinement, and the difference between both are shown in Fig. 2. The left inset of this figure shows the magnification near the peaks at 37°. The right inset shows how lattice parameters vary as a function of the starting composition y in the MoO_y.

The Rietveld refinement was performed using GSAS-EXPGUI program [24, 25], and the starting data chosen for this refinement was published by Bolzan et al. [26] for the MoO_2. The refinement were stable and yielded the lattice parameters a=5.603(3) Å, b=4.855(4) Å, c=5.624(6) Å, $\alpha=\gamma=90°$, and β=120.929(2)° which are in good agreement with previous work [25]. The goodness of fit was S (R_{wp}/

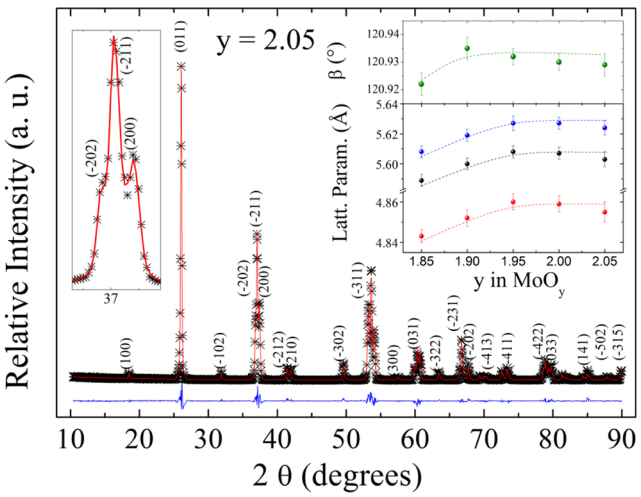

Fig. 2 X-ray powder diffraction pattern (*asterisks*), final Rietveld refinement (*red lines*), and difference between both (*blue line*) for a sample with starting composition of $MoO_{2.05}$. *Left inset* shows the magnification near the peaks at 37°. *Right inset* shows how lattice parameters vary as a function of the starting composition y in the MoO_y. *Dashed lines* are guides by the eyes

R_{exp})=1.57. Left inset shows small changes in the 1.85 to 1.95 range. Above y=1.95, the changes cannot be accounted because they are within the error bar.

In Fig. 3, one can observe that the R(T) curves are dependent on the starting oxygen composition for single-phase samples. For y=1.95, 2.00, and 2.05, a metal-insulator transition occurs close to 110 K. Furthermore, a second transition from semiconducting to metallic is observed near 25 K in these samples. The origin of the transitions in the MoO_y is still under discussion but seems to be strongly reminiscent of those observed in η-Mo_4O_{11} which are generally assigned to the CDW instabilities [14]. Inset displays electrical resistance as a function of temperature of a sample with low oxygen content (y=1.85). This behavior is different from what is expected for conventional metals. A similar anomalous behavior has been reported recently by us for the K_xMoO_2 compound. A power-law of $R(T)\sim T^{\alpha}$, with α=0.46(8), has fitted this result. For the best of our knowledge, this is the first time that this anomalous behavior has been observed in MoO_2. It is important to mention that the sample with starting composition of MoO_2 does not exhibit the metal-like behavior published for MoO_2 [4, 20] due to methodology adopted in this work which does not provide a precise control of the molybdenum valences in the same sample. So, let us discuss the influence that valences can have on the electronic properties of MoO_y samples.

Core level photoemission spectroscopy for the MoO_y samples with 1.85≤y≤2.05 is displayed in Fig. 4.

The Mo 3p core level spectra, shown in Fig. 4, display two main structures associated with the Mo $3p_{3/2}$ and Mo $3p_{1/2}$ levels which are split due to spin-orbit effects. In the Mo $3p_{3/2}$ region, the peak around 398.5 eV is assigned to Mo^{4+} ($4d^2$) states, but there is also a Mo^{3+}($4d^3$) contribution near 395.5 eV. In the Mo $3p_{1/2}$ region, the peaks are near 415 and 413 eV, respectively,

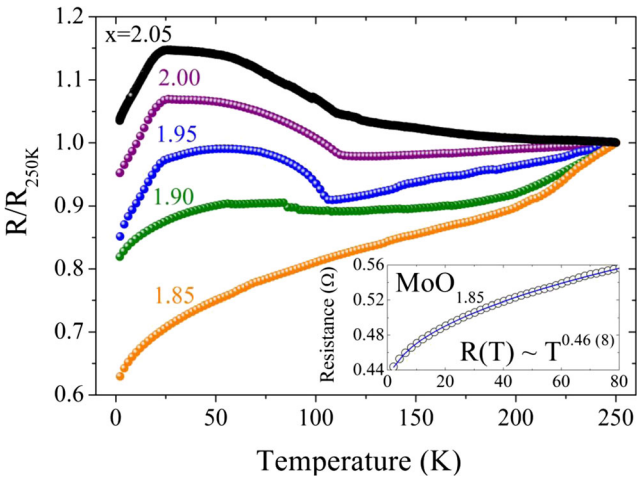

Fig. 3 R/R_{250K} as a function of temperature for samples with starting composition MoO_y in the 1.85≤y≤2.05 range. *Inset* shows electrical resistance as a function of temperature for a sample with starting composition $MoO_{1.85}$ displaying power-law behavior. *Blue line* indicates a fitting with $R(T)=T^{\alpha}$ with α=0.46(8)

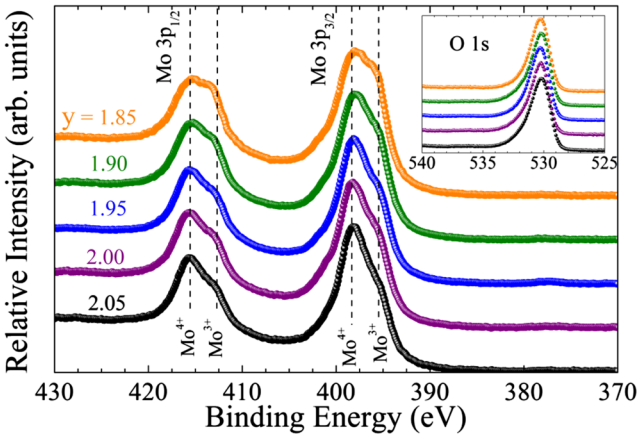

Fig. 4 Mo 3p core level photoemission (XPS) spectra of MoO_y samples with 1.85≤y≤2.00. *Inset* shows the O 1s core level XPS of MoO_y samples

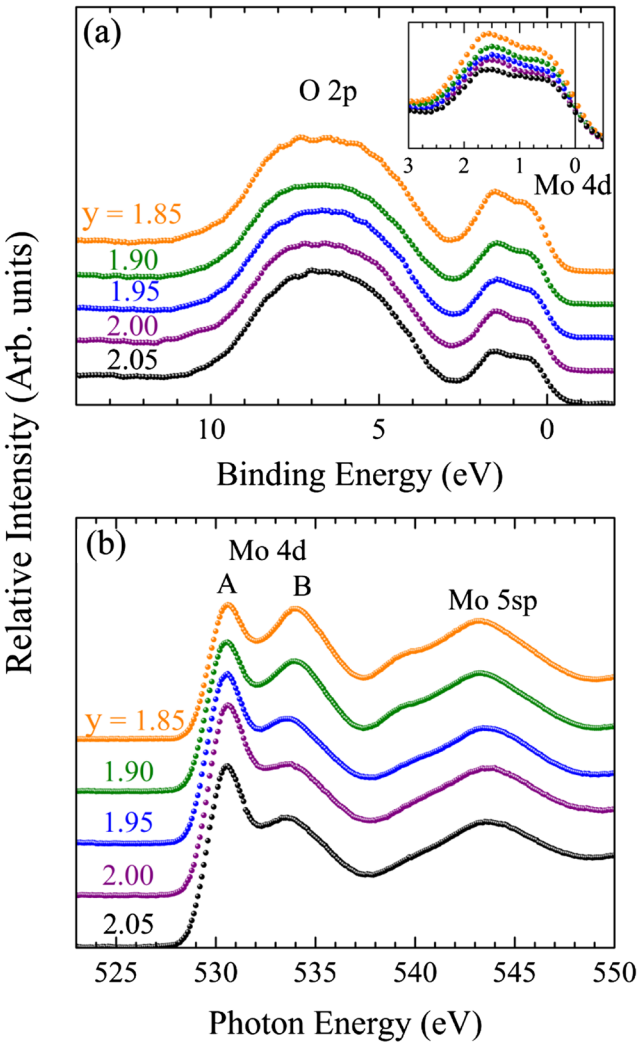

Fig. 5 **a** Valence band photoemission spectra of MoO_y samples with 1.85≤y≤2.00. The *inset* shows the change in intensity in the region near the Fermi level in better detail. **b** O 1s X-ray absorption spectra of MoO_y samples with 1.85≤y≤2.00

due to Mo^{4+} and Mo^{3+} ions. Similar discussion has been addressed recently by us for the K_xMoO_2 compound [19, 20]. Furthermore, reference 20 shows that the metal-like behavior is observed in the MoO_2 compound when Mo^{3+} content vanishes. The inset also shows the O 1s core level spectra for the MoO_y samples. The single-peak structure does not change as a function of y showing that the oxygen states remain unaffected by its stoichiometry (by this composition).

The electron doping caused by the amount of oxygen in each sample also affects the valence and conduction states. Figure 5a shows the valence band photoemission spectra for the MoO_y samples. All the spectra are formed by the O 2p band, from about 10 to 3.0 eV, and the Mo 4d band, from around 3.0 to 0 eV. More importantly, the inset shows that, as the oxygen content decreases, the intensity of the Mo 4d band becomes relatively larger. This can be interpreted as an increase of the electron count in the Mo 4d states.

Conversely, Fig. 5b presents the O 1s X-ray absorption spectra for the MoO_y samples. This technique is related to transitions from the O 1s core level to empty O 2p states. Therefore, the spectra is related to the O 2p conduction band, covalently mixed with Mo 4d states, from 528 to 537 eV, and with Mo 5s and 5p states, above 537 eV. The main change here, as a function of y, is the decrease in the relative intensity of the first peak in the Mo 4d region (peak A). This can be related with a decrease in the unoccupied density of states, just above the Fermi level. Again, the changes in the spectra point to an increase in the electron count in the Mo 4d states.

The results show that the samples with several oxygen compositions have different Mo^{3+}/Mo^{4+} contributions. Particularly, the reduced oxygen stoichiometry increases the Mo^{3+} contribution, inducing an electron doping effect. Thus, there is a direct correlation between the electron doping in the sample and the observation of metal-insulator transition and the anomalous power-law behavior. Furthermore, no K-doping is necessary for the appearance of the anomalous power-law behavior observed in MoO_y and K_xMoO_2 [19, 20].

4 Conclusions

XRD shows that the MoO_y samples are single phase within the limit $1.85 \leq y \leq 2.05$. Electrical resistivity measurements are very sensitive to the oxygen composition. When the Mo^{3+}/Mo^{4+} ratio is high, samples show various unexpected electrical behaviors. Samples with $y=1.85$ and 1.90 display anomalous power-law behavior suggesting a low-dimensional electrical conductivity similarly to the K_xMoO_2 compound. Core level photoemission, valence band photoemission, and X-ray absorption results show that these samples have different concentration of Mo^{3+} ions. The results unambiguously show that the presence of Mo^{3+} ions is necessary for inducing the power-law behavior observed in the MoO_y and K_xMoO_2 compounds.

Acknowledgments This material is based upon work supported by the CNPq (508308/2010-0, 309084/2010-5, 448041/2014-6, 300821/2012-3, and 490182/2009-7) and FAPESP (2009/14524-6, 2009/54001-2, and 2010/06637-2); M.S. da Luz also thanks CAPES and FAPEMIG.

References

1. L. Kihlborg, Acta Chem. Scand. **13**, 954 (1959)
2. H. Gruber, H. Haselmair, H.P. Fritzer, J. Solid State Chem. **47**, 84 (1983)
3. M. Greenblatt, Chem. Rev. **88**, 31 (1988)
4. L. Bendor, Y. Shimony, Mater. Res. Bull. **9**, 837 (1974)
5. P. Thakur, J.C. Cezar, N.B. Brookes, R.J. Choudhary, R. Prakash, D.M. Phase, K.H. Chae, R. Kumar, Appl. Phys. Lett. **94**, 062501 (2009)
6. J. Nisar, X. Peng, R. Ahuja, Phys. Rev. B **81**, 012402 (2010)
7. F. Wang, Z. Pang, L. Lin, S. Fang, Y. Dai, S. Han, Phys. Rev. B **81**, 134407 (2010)
8. B.G. Brandt, A.C. Skapski, Acta Chem. Scand. **21**, 661 (1967)
9. V. Eyert, R. Horny, K.H. Hock, S. Horn, J. Phys. Condens. Matter **12**, 4923 (2000)
10. D.O. Scanlon, G.W. Watson, D.J. Payne, G.R. Atkinson, R.G. Egdell, D.S.L. Law, J. Phys. Chem. C **114**, 4636 (2010)
11. G. Andersson, A. Magneli, Acta Chem. Scand. **4**, 793 (1950)
12. M. Sato, H. Fujishita, S. Sato, S. Hoshino, J. Phys. C: Solid State Phys **19**, 3059 (1986)
13. M. Sato, M. Onoda, Y. Matsuda, J. Phys. C: Solid State Phys **20**, 4763 (1987)
14. H. Guyot, C. Escribefilippini, G. Fourcaudot, K. Konate, C. Schlenker, J. Phys. C: Solid State Phys **16**, 1227 (1983)
15. M.S. da Luz, J.J. Neumeier, C.A.M. dos Santos, B.D. White, H.J. Izario Filho, J.B. Leao, Q. Huang, Phys. Rev. B **84**, 014108 (2011)
16. M.P. Nikiforov, A.F. Isakovic, D.A. Bonnell, Phys. Rev. B **76**, 033104 (2007)
17. H.M. Tsai, K. Asokan, C.W. Pao, J.W. Chiou, C.H. Du, W.F. Pong, M.H. Tsai, L.Y. Jang, Appl. Phys. Lett. **91**, 022109 (2007)
18. C.A.M. dos Santos, M.S. da Luz, Y.-K. Yu, J.J. Neumeier, J. Moreno, B.D. White, Phys. Rev. B **77**, 193106 (2008)
19. L.M.S. Alves, V.I. Damasceno, C.A.M. dos Santos, A.D. Bortolozo, P.A. Suzuki, H.J. Izario Filho, A.J.S. Machado, Z. Fisk, Phys. Rev. B **81**, 174532 (2010)
20. L.M.S. Alves, C.A.M. dos Santos, A.J.S. Machado, B.S. de Lima, J.J. Neumeier, M.D.R. Marques, J.A. Aguiar, R.J.O. Mossanek, M. Abbate, J. Appl. Phys. **112**, 073923 (2012)
21. C. Schlenker, H. Schwenk, C. Escribefilippini, J. Marcus, Physica B C **135**, 511 (1985)
22. D. Parker, J.C. Idrobo, C. Cantoni, A.S. Sefat, Phys. Rev. B **90**, 054505 (2014)
23. H.-K. Fun, P. Yang, M. Sasaki, M. Inoue, H. Kadomatsu, Acta Crystallogr C **55**, 841–843 (1999)
24. A.C. Larson and R.B. Von Dreele, General Structure Analysis System (GSAS), Los Alamos National Laboratory Report LAUR 86-748 (1994)
25. B.H. Toby, J. Appl. Crystallogr. **34**, 210 (2001)
26. A.A. Bolzan, B.J. Kennedy, C.J. Howard, Aust. J. Chem. **48**, 1473 (1995)